acyl-lysophosphatidic acids) from phospholipids (*16*, *17*). LPA has been described as an extracellular mediator of many biological functions, such as proliferation, antiapoptotic activity, and cytoskeletal organization, and appears to signal through at least five members of a family of G protein–coupled receptors (*12*, *17*–*22*). Lipase H is highly homologous to lipase I (*LIPI*) and phosphatidylserine-specific phospholipase A1 (*PS-PLA1*). These three proteins also share common structures of short lid domains and partially deleted β9 loop domains that probably determine the specificity of their phospholipase activity in the production of LPA (*14*, *23*) (figs. S7 and S9).

To elucidate whether the *LIPH* gene is expressed in hair follicle development, we analyzed mRNA transcripts isolated from human hair follicles and other tissues. The expression of *LIPH,* but not *LIPI* and *PS-PLA1*, was prominent in hair follicles, including the stem cell–rich bulge region (Fig. 3 and fig. S8). These data further indicate the importance of *LIPH* in normal hair formation and growth.

The physiological function of LIPH has not yet been elucidated. We speculate that intragenic deletion of the *LIPH* (loss-of-function mutation) abolishes the enzymatic activity of lipase H and diminishes the production of LPA mediators in hair follicles. Such lipid mediators may affect the migration, differentiation, or proliferation of keratinocytes, culminating in arrest of hair growth (fig. S9). However, LPA-independent mechanisms and other activities, for example, intracellular functioning of LIPH, cannot be ruled out. Like age-related hair loss in the general population, the hypotrichosis and alopecia described here are not associated with other pathologies, and they progress with age. The identification of a genetic defect in *LIPH* suggests that this enzyme regulates hair growth and therefore may be a potential target for the development of a therapeutic agent for the control of hair loss or growth.

References and Notes

1. R. Paus, G. Cotsarelis, *N. Engl. J. Med.* **341**, 491 (1999).
2. G. Cotsarelis, T. T. Sun, R. M. Lavker, *Cell* **61**, 1329 (1990).
3. S. Lyle *et al.*, *J. Cell Sci.* **111**, 3179 (1998).
4. K. A. Moore, I. R. Lemischka, *Science* **311**, 1880 (2006).
5. W. Ahmad *et al.*, *Science* **279**, 720 (1998).
6. A. Kljuic *et al.*, *Cell* **113**, 249 (2003).
7. E. Levy-Nissenbaum *et al.*, *Nat. Genet.* **34**, 151 (2003).
8. E. I. Rogaev, R. A. Zinchenko, G. Dvoryachikov, T. Sherbatich, E. K. Ginter, *Lancet* **354**, 1097 (1999).
9. Online Mendelian Inheritance in Man, OMIM database 604379 (www.ncbi.nlm.nih.gov/entrez/dispomim.cgi?id=604379).
10. E. S. Lander *et al.*, *Nature* **409**, 860 (2001).
11. W. Jin, U. C. Broedl, H. Monajemi, J. M. Glick, D. J. Rader, *Genomics* **80**, 268 (2002).
12. H. Sonoda *et al.*, *J. Biol. Chem.* **277**, 34254 (2002).
13. M. Hiraoka, A. Abe, J. A. Shayman, *J. Lipid Res.* **46**, 2441 (2005).
14. T. Hiramatsu *et al.*, *J. Biol. Chem.* **278**, 49438 (2003).
15. R. J. Kubiak *et al.*, *Biochemistry* **40**, 5422 (2001).
16. J. Aoki *et al.*, *Biochim. Biophys. Acta* **1582**, 26 (2002).
17. J. Aoki, *Semin. Cell Dev. Biol.* **15**, 477 (2004).
18. K. Bandoh *et al.*, *J. Biol. Chem.* **274**, 27776 (1999).
19. F. N. van Leeuwen, B. Giepmans, L. van Meeteren, W. Moolenaar, *Biochem. Soc. Trans.* **31**, 1209 (2003).
20. G. A. Piazza, J. L. Ritter, C. A. Baracka, *Exp. Cell Res.* **216**, 51 (1995).
21. W. H. Moolenaar, L. A. van Meeteren, B. N. Giepmans, *Bioessays* **26**, 870 (2004).
22. S. Choi, M. Lee, A. L. Shiu, S. J. Yo, G. W. Aponte, *Am. J. Physiol. Gastrointest. Liver Physiol*., published online 24 August 2006, 10.1152/ajpgi.00295.2006.
23. F. Carriere *et al.*, *Biochim. Biophys. Acta* **1376**, 417 (1998).

24. We thank the study participants; colleagues who assisted in evaluation of the patients; V. Nikishina and O. Plotnikova for technical support; and S. Borinskaya, N. Yankovsky, and E. Khusnutdinova for providing some of the population DNA samples. The project was supported in part by a program of the Presidium of the Russian Academy of Sciences, "Biodiversity and Dynamics of Gene Pools" (to E.I.R.). S.L. was supported by NIH K08-AR02179 and the Ellison Medical Foundation. The collection of blood samples was approved by the Institutional Review Board (IRB) and Ethical Committee of the Center of Medical Genetics (Moscow), with informed consent obtained from all affected individuals and their relatives.

Supporting Online Material

www.sciencemag.org/cgi/content/full/314/5801/982/DC1
Materials and Methods
SOM Text
Figs. S1 to S10
Table S1
References

1 August 2006; accepted 6 October 2006
10.1126/science.1133276

Microtubule-Severing Activity of *Shigella* Is Pivotal for Intercellular Spreading

Sei Yoshida,[1,4] Yutaka Handa,[1,4] Toshihiko Suzuki,[1,4] Michinaga Ogawa,[1,4] Masato Suzuki,[1,4] Asuka Tamai,[5] Akio Abe,[5] Eisaku Katayama,[2] Chihiro Sasakawa[1,3,4]*

Some pathogenic bacteria actually invade the cytoplasm of their target host cells. Invasive bacteria acquire the propulsive force to move by recruiting actin and inducing its polymerization. Here we show that *Shigella* movement within the cytoplasm was severely hindered by microtubules and that the bacteria destroyed surrounding microtubules by secreting VirA by means of the type III secretion system. Degradation of microtubules by VirA was dependent on its α-tubulin–specific cysteine protease–like activity. *virA* mutants did not move within the host cytoplasm and failed to move into adjacent cells.

Cytoplasm-invading pathogens, including *Shigella* (*1*–*3*), *Listeria monocytogenes* (*4*–*6*), the spotted-fever group *Rickettsia* (*7*–*9*), *Mycobacterium marinum* (*10*), and *Burkholderia pseudomallei* (*11*, *12*), induce local actin polymerization at one pole of the bacterium, which gives them the propulsive force to move within the cytoplasm and into adjacent host cells, an important bacterial activity for establishing an infectious foothold and for renewing replicative niches. Although the bacterial proteins involved in mediating actin polymerization differ, they share the ability to recruit and activate actin-related proteins 2 and 3 in complex (Arp2/3) in the vicinity of the bacterial surface, which induces local actin polymerization (*13*–*15*). The actin-based motility of *Shigella* is mediated by the special interplay between an outer membrane protein, VirG (IcsA), and the neural Wiskott-Aldrich syndrome protein (N-WASP) (*16*, *17*). When VirG and Cdc42 bind to N-WASP, N-WASP becomes activated and, in turn, recruits the Arp2/3 complex (*17*, *18*).

The rate of motility and direction of movement of pathogens within the host cytoplasm, however, is highly variable and depends on the stage of bacterial multiplication and location in the host cell (*19*). The bacterial movement behavior of motile *Shigella* is heterogeneous: Some bacteria suddenly change direction, spin around, or stop moving within the cytoplasm, independent of bacterial division (fig. S1) (*20*), whereas bacterial movement at the perinuclear surface or along the periphery of the cytoplasm tends to proceed smoothly and rapidly, which suggests that some intracellular structure, such as a subcellular organelle or the cytoskeleton, influences the rate of motility. This notion is supported by studies on *L. monocytogenes*, whose movement in host cells is affected by a subcellular organelle and the cytoskeleton (*21*).

VirA is a *Shigella* effector, secreted by means of the type III secretion system (TTSS), that is

[1]Department of Microbiology and Immunology, [2]Department of Basic Medical Sciences, [3]Department of Infectious Control, International Research Center for Infectious Diseases, Institute of Medical Science, University of Tokyo, 4-6-1, Shirokanedai, Minato-ku, Tokyo 108-8639, Japan. [4]CREST, Japan Science and Technology Corporation (JST). 4-1-8, Honche, Kawaguchi-shi, Saitama 332-0012, Japan. [5]Laboratory of Bacterial Infection, Kitasato Institute for Life Science, Kitasato University, 5-9-1 Shirokane, Minato-ku, Tokyo 108-8641, Japan.

*To whom correspondence should be addressed. E-mail: sasakawa@ims.u-tokyo.ac.jp

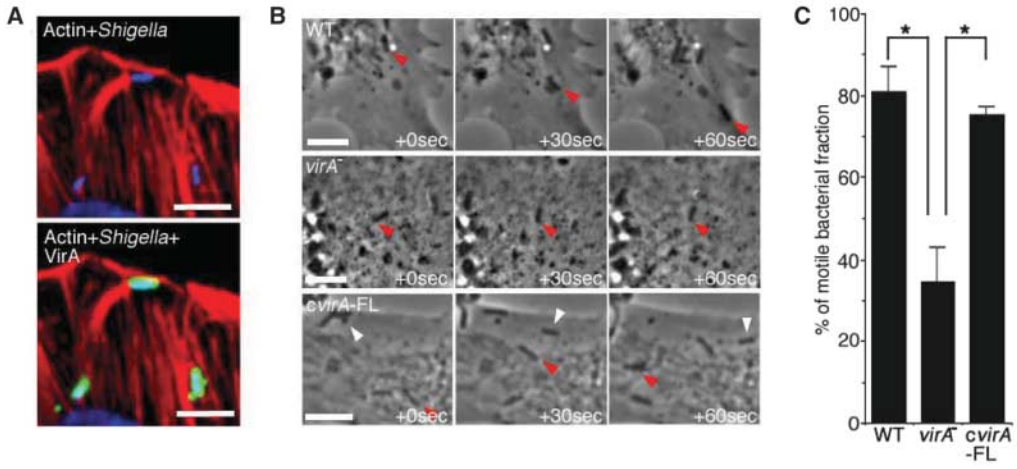

Fig. 1. VirA activity facilitates bacterial movement. (**A**) COS-7 cells were infected with *Shigella* and stained for DNA with TOPRO-3 to identify the bacteria (blue), with rhodamine-phalloidin for actin (red) and with a VirA-specific antibody for VirA (green). Scale bar, 5 μm. (**B**) COS-7 cells were infected with the WT (WT), the *virA* mutant (*virA*$^{-}$), or the full-length VirA complementation strain (c*virA*-FL), and the movement of each strain in the cells was observed. Arrowheads indicate bacteria. Scale bar, 5 μm. (**C**) The fraction of motile bacteria was investigated and its percentage was calculated. *$P < 0.05$.

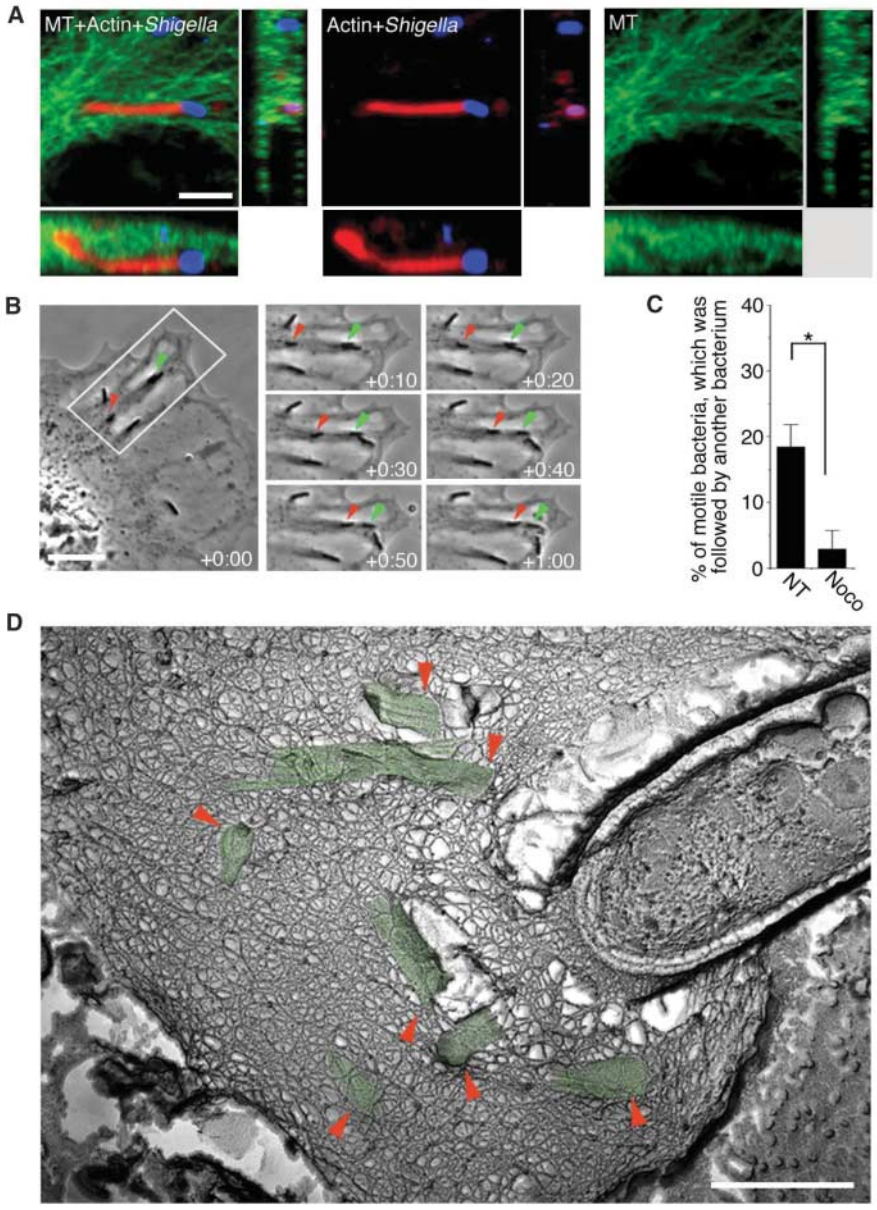

Fig. 2. *Shigella* destroys the host MT network during spreading. (**A**) COS-7 cells were infected with the WT and stained with rhodamine-phalloidin (actin, red), an antibody against *S. flexneri* lipopolysaccharide (*Shigella*, blue), and an antibody against α-tubulin (MT, green). Scale bar, 5 μm. (**B**) COS-7 cells were infected with WT, and the bacterial movement of each in the cells was observed. Arrowheads indicate bacteria. Scale bar, 5 μm. (**C**) Nocodazole-treated (Noco) and untreated (NT) cells were infected. The fraction of motile bacteria under each condition was investigated and its percentage was calculated. *$P < 0.05$. (**D**) FFEM image of the *Shigella*-induced F-actin network and destroyed MTs (red arrowheads, green) in COS-7 cells. Scale bar, 0.2 μm.

required for entry into epithelial cells and subsequent intra- and intercellular spreading (*22*). VirA can interact with the α,β-tubulin heterodimer and can induce microtubule (MT) destabilization in vitro and in vivo (*23*, *24*). VirA expression by *Shigella* is highly responsive to intracellular conditions (*22*, *25*), and *virA* mutants fail to disseminate into adjacent cells, which suggests that VirA plays a pivotal role in promoting the intra- and intercellular spreading of *Shigella* (*22*).

To clarify the role of VirA in the intracellular *Shigella* motility process, we localized VirA secreted by intracellular wild-type *Shigella* (WT) by immunofluorescence microscopy. Around 80 min after bacterial invasion of COS-7 cells, VirA signals were detected on the motile bacterial surface, which formed a long actin tail at one pole of the bacterium (Fig. 1A). We used time-lapse photography to investigate the intracellular behavior of the WT, c*virA*-FL (the *virA* gene was replaced with a cloned full-length *virA* gene), and the *virA* mutant (*virA*$^-$). Although both the WT and c*virA*-FL moved smoothly, *virA*$^-$ occasionally changed direction but did not move (Fig. 1B). Around 80 min after invasion, the *virA* mutant, like the WT, formed a long actin tail (fig. S2A), which suggested that the defect in the motility of *virA*$^-$ was not directly related to the VirG activity required for formation of the actin tail. At this stage of infection, about 80% of the WT and c*virA*-FL were motile, whereas only about 30% of the intracellular *virA* mutant were motile (Fig. 1, B and C). Thus, VirA activity is pivotal for promotion of bacterial motility.

To determine whether cytoplasmic MT structures act as a physical barrier to bacterial movement, COS-7 cells pretreated with the MT-destabilizing drug nocodazole were infected with the *virA* mutant. Although the motile WT population in COS-7 cells treated with or without nocodazole was ~60%, the motile *virA* mutant population in the cells treated with nocodazole was as high as ~60%, compared with ~20% in the untreated cells (fig. S2, B and C). The movement of the WT in the COS-7 cells occasionally followed a zigzag path. At some point the bacterial movement would stop, and the bacteria would change direction (+20 and 30 s) and continue to move within the cytoplasm (+40 s) (fig. S1A). The bacterial movement in cells pretreated with nocodazole, however, became smooth (fig. S1B). Bacterial movement in the cytoplasm of COS-7 treated with nocodazole tended to proceed smoothly by sliding, without stopping, in contrast to the movement in the cells not treated with nocodazole. The highest speed in the cells not treated with nocodazole was 0.68 μm/s, and the slowest speed was 0.08 μm/s (fig. S1C), whereas the highest speed in the cells treated with nocodazole was 0.48 μm/s, and the lowest speed was 0.13 μm/s (fig. S1D). Clearly, the speed with which *Shigella* moved in the cytoplasm exhibited greater variation in cells not treated with nocodazole. The standard deviation of the speed of the WT in the untreated cells was significantly greater than in the cells treated with nocodazole (fig. S1E). By contrast, when COS-7 cells were treated with taxol, an agent that freezes MT instability, the distribution of the standard deviation of the bacterial speed in COS-7 cells was not substantially different (fig. S1F).

To further characterize bacterial movement within the cytoplasm, we examined COS-7 cells infected with WT by immunofluorescence confocal microscopy, 80 min after invasion. In some areas of bacterial movement within the cytoplasm, MTs were lacking (Fig. 2A). The tunnel-like area created through the MT networks behind the bacteria corresponded to the area where the actin tail of the motile bacterium had formed (Fig. 2A and fig. S3). A tunnel-like area created behind motile *Shigella* was also observed in other cell lines (fig. S3). When we viewed motile bacteria by time-lapse photography, they occasionally followed the same course as created by the bacterium ahead of them (Fig. 2B). After 80 to 120 min after invasion, ~20% of motile bacteria were followed by another bacterium along the same course, whereas only 3% of motile bacteria in the cells pretreated with nocodazole were followed by another bacterium along the same course (Fig. 2C). Thus, the tunnel created by the first motile bacterium facilitates the movement of the second. We then performed freeze-fracture electron microscopy (FFEM) to further characterize the tunnel-like zone visualized by MT staining (*20*). Fragmented structures (Fig. 2D) were frequently detected within the actin tail created by motile *Shigella*, which resembled the characteristic MT structure (see also below); this observation strongly suggested that motile *Shigella* could break down surrounding MTs as it moves. Indeed, when motile *Shigella* were quadruple stained for F-actin, bacterium, MTs, and VirA and examined by confocal immunofluorescence microscopy, the VirA signal was detected on the bacterial surface, where the local MTs surrounding the bacterium had been destroyed (fig. S4).

The VirA-treated MTs underwent severe segmentation and appeared much rougher than the MTs incubated with buffer alone (Fig. 3, A and B). Both the VirA-treated MTs and the fragmented structures detected in the *Shigella* actin tail were composed of six strips, a characteristic of MTs (Fig. 3, B to D), which suggests that the VirA protein secreted by motile *Shigella* was involved in breaking down the surrounding MTs as the bacteria moved.

Because the distinctive two-dimensional structure resembled that of a group of cysteine peptidases known as the Clan CA family (Fig. 4A) (*26*, *27*), we investigated whether VirA acts

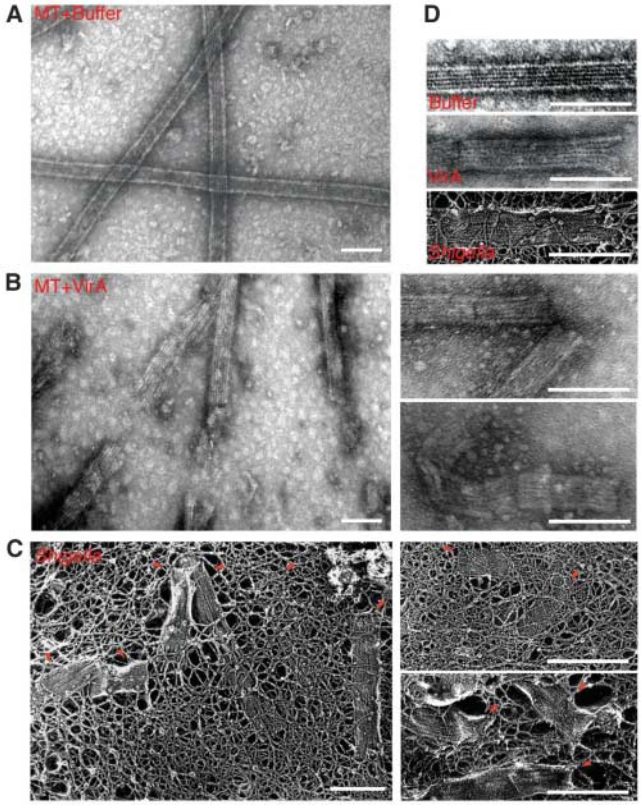

Fig. 3. VirA secreted from motile *Shigella* destroys surrounding MTs. (**A**) Electron microscopic (EM) image of the MTs in vitro. (**B**) EM images of the VirA-treated MTs in vitro. (**C**) FFEM images of the *Shigella*-induced F-actin network and destroyed MTs (red arrowheads) in COS-7 cells. (**D**) Comparison between the EM image of the VirA-treated MTs (middle) and FFEM image of *Shigella*-induced MT destruction (bottom). EM image of MTs treated with buffer alone (top) as a control. The twice-cycled MT proteins that contained MAPs (microtubule-associated proteins, known as MT-stabilizing factors) prepared from bovine brain lysates were used in (A) and (B). After inducing the polymerization, MTs were incubated with VirA proteins, which were purified from the glutathione *S*-transferase fusion protein GST-VirA, in PIPES-based buffer containing 1.3 M glycerol (*23*) at 37°C for 30 min, and analyzed by EM (*20*, *23*). Scale bar, 0.1 μm.

as a cysteine protease. β-Tubulin was reproducibly precipitated by VirA-specific antibody, but α-tubulin was not (Fig. 4B) (*23*). α-Tubulin was highly degraded, but β-tubulin was not degraded at all, when tubulin was incubated with VirA-FL (full-length VirA) in the protease buffer for 120 min (Fig. 4, C and D). To confirm the cysteine protease–like activity of VirA, cysteine 34 was replaced by serine (VirA-C34S), and VirA-C34S was tested for its ability to degrade α-tubulin by incubating tubulin heterodimer under the same conditions. The immunoprecipitation assay with VirA-specific antibody indicated that both α-tubulin and β-tubulin interacted with VirA-C34S but that α-tubulin was degraded less efficiently than VirA-FL (Fig. 4B). Indeed, when tubulin was incubated with VirA-FL or VirA-C34S in the protease buffer for 120 min, VirA-FL resulted in greater degradation of α-tubulin than VirA-C34S (Fig. 4E). When leupeptin, a serine and cysteine protease inhibitor, was added to the assay medium under the same conditions, VirA-FL activity was completely inhibited (Fig. 4F). Although less effective than leupeptin, another cysteine protease inhibitor, cystatin C, also inhibited the degradation of α-tubulin by VirA

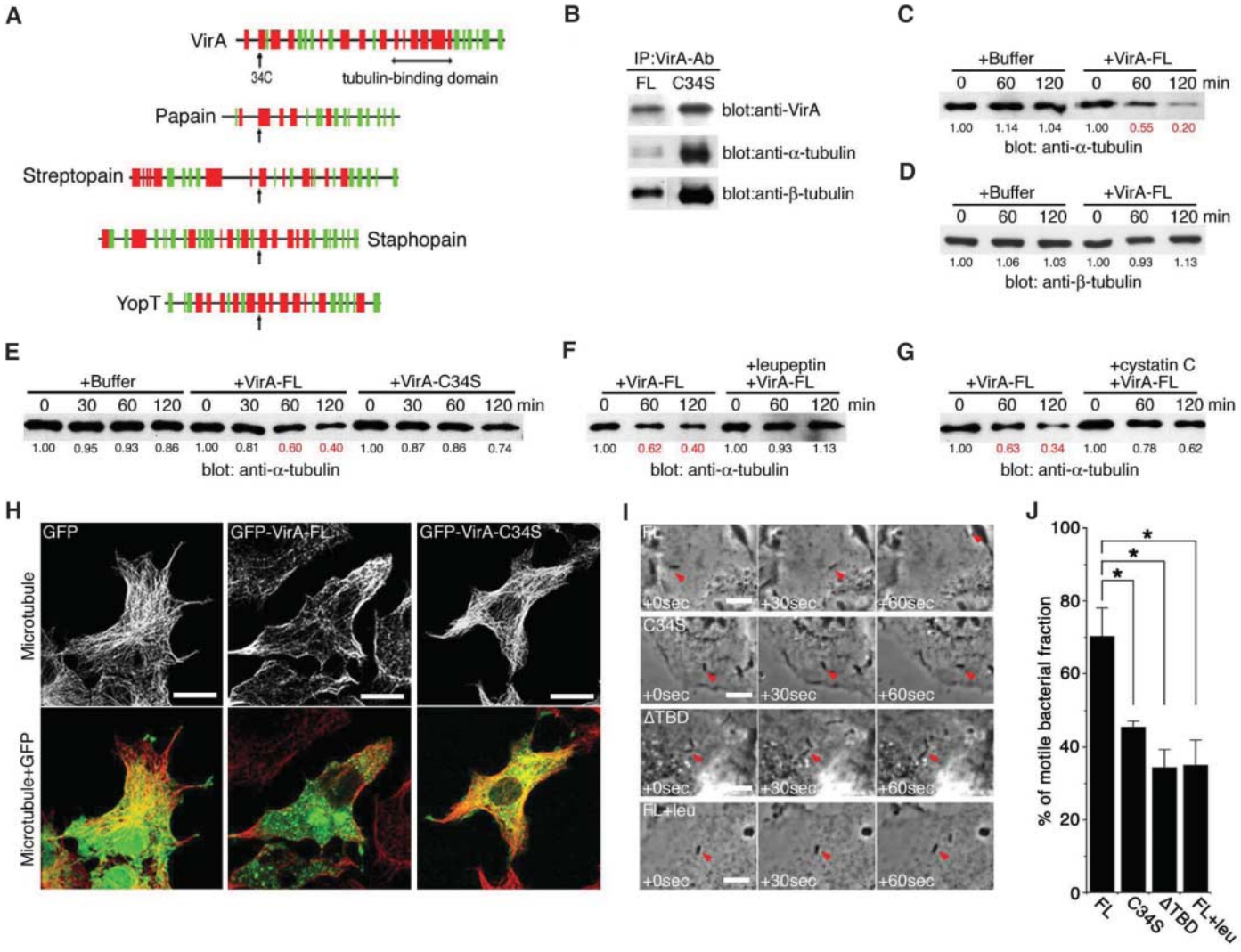

Fig. 4. VirA has cysteine protease–like activity and a critical cysteine residue. (**A**) Comparison of the secondary structure profile of VirA and of the CA clan of cysteine proteases, papain, streptopain, staphopain, and YopT, using the 3D-PSSM protein folding recognition server (*30*). The red box represents the α helix, and the green box represents the β sheet. "34C" indicates Cys^{34}, which is located at the start of a major α helix. (**B**) Purified human tubulin (0.5 μM) (HeLa cells) heterodimer (composed of α- and β-tubulin) was mixed with purified VirA-FL (1 μM) or VirA-C34S (1 μM) in a protease assay buffer [20 mM Hepes, pH 7.4, 10 mM DTT, 0.1% CHAPS, 10% sucrose, 1 mM 4-(2-aminoethyl) benzenesulfonyl fluoride hydrochloride (AEBSF)] on ice. After incubation at 37°C for 3 hours, the mixture was immunoprecipitated with VirA-specific antibody at 4°C overnight, and the immunoprecipitates were subjected to immunoblotting. (**C**) After mixing 1 μM tubulin and 1 μM VirA-FL, they were incubated at 37°C for 60 or 120 min, and samples were analyzed by immunoblotting with an antibody against α-tubulin. (**D**) Same as in (C), but an antibody against β-tubulin was used. The numbers below the images are the result of the NIH image analysis. (**E**) After mixing 1 μM tubulin with 1 μM VirA-FL or 1 μM VirA-C34S, the mixture was incubated at 37°C for 60 or 120 min, and analyzed by immunoblotting with an antibody against α-tubulin. The blots were quantified by measuring relative intensity with NIH-image software version 1.63, and the values are indicated below the images. (**F** and **G**) After mixing 1 μM tubulin, 1 μM VirA-FL, and leupeptin (100 μg/ml) (F) or cystatin C (1 μM) (G) in a plastic well, they were incubated at 37°C for 60 or 120 min and analyzed by immunoblotting with an antibody against α-tubulin. The numbers below the images are the results of NIH image analysis. (**H**) GFP–VirA-FL or GFP–VirA-C34S was expressed in COS-7 cells. After fixation, the cells were subjected to immunofluorescence staining. Scale bar, 10 μm. (**I**) COS-7 cells were infected with *cvirA*-FL (FL), *cvirA*-C34S (C34S), and *cvirA*-ΔTBD (ΔTBD); leupeptin-treated COS-7 cells were infected with *cvirA*-FL (FL+leu). Movement of each of the bacteria in the cells was observed. Arrowheads indicate bacteria. Scale bar, 5 μm. (**J**) The percentage of the motile bacterial fraction of (I) was calculated. *$P < 0.05$.

(Fig. 4G). To confirm the effect of the substitution of serine for cysteine 34 on VirA activity in vivo, we investigated the MT structure of COS-7 cells transfected with green fluorescent protein pGFP–VirA-FL or pGFP–VirA-C34S (*20*). The MT networks were severely disrupted in the COS-7 cells transiently expressing GFP–VirA-FL, but not in those expressing GFP–VirA-C34S (Fig. 4H). Indeed, when cell lysates containing GFP–VirA-FL or GFP–VirA-C34S were pulled down by GFP-specific antibody, more α-tubulin and β-tubulin were precipitated by GFP–VirA-C34S than by GFP–VirA-FL. Consistent with these results, time-lapse photography showed that the motility rate of *Shigella* expressing VirA-C34S (c*virA*-C34S, the VirA-C34S complementation strain) in COS-7 cells was less than that of c*virA*-FL (Fig. 4, I and J). Because the portion of VirA encompassing residues 224 through 315 [tubulin-binding domain (TBD)] (Fig. 4A) has been shown to be involved in interaction with tubulin in vitro (*23*), we created a VirA-ΔTBD complementation strain (c*virA*-ΔTBD) and investigated intracellular movement. The bacterial motility rate of c*virA*-ΔTBD was further decreased compared with that of c*virA*-C34S (Fig. 4, I and J). It was also decreased when the cells were treated with leupeptin (Fig. 4, I and J), which demonstrated that VirA-protease–like activity was important for promoting intracellular bacterial movement.

To establish the in vivo role of VirA in bacterial infection, C57BL/6 mice were intranasally infected with 5×10^7 CFU of the WT, the *virA*$^-$, c*virA*, c*virA*-C34S, or TTSS-deficient mutant (*20*). Each mouse was weighed after bacterial infection, and the survival rate was calculated (fig. S5). Although 100% of the mice were killed by the WT by day 9, none were killed by the *virA*$^-$ or TTSS-deficient mutant. Although 100% of the mice were killed by c*virA* under the same conditions, only 60% were killed by c*virA*-C34S. Thus, the VirA activity that degrades MT contributes to *Shigella*'s pathogenicity and that the cysteine 34 of VirA is a crucial residue for its activity.

It is noteworthy that *L. monocytogenes* can recruit Op18 (stathmin), an MT-sequestering host protein (*28*), in the vicinity of the bacterial surface in infected host cells (*29*). Perhaps the Op18 recruited by intracellular *L. monocytogenes* causes local destruction of MTs surrounding the bacterium, and that facilitates bacterial movement.

In conclusion, the ability of VirA to degrade MTs by means of cysteine protease–like activity is critical to the intra- and intercellular spreading by intracellular *Shigella* that leads to bacillary dysentery, even though host-cell MT structures obstruct bacterial movement (fig. S6).

References and Notes

1. S. Makino, C. Sasakawa, K. Kamata, M. Yoshikawa, *Cell* **46**, 551 (1986).
2. M. L. Bernardini, J. Mounier, H. D'Hauteville, P. J. Sansonetti, *Proc. Natl. Acad. Sci. U.S.A.* **86**, 3867 (1989).
3. M.-C. Lett *et al.*, *J. Bacteriol.* **171**, 353 (1989).
4. L. G. Tilney, D. A. Portonoy, *J. Cell Biol.* **109**, 1597 (1989).
5. E. Domann *et al.*, *EMBO J.* **11**, 1981 (1992).
6. C. Kocks *et al.*, *Cell* **68**, 521 (1992).
7. N. Teysseire, C. Chiche-Portiche, D. Raoult, *Res. Microbiol.* **143**, 821 (1992).
8. R. A. Heinzen, S. F. Hayes, M. G. Peacock, T. Hackstadt, *Infect. Immun.* **61**, 1926 (1993).
9. E. Gouin *et al.*, *Nature* **427**, 457 (2004).
10. L. M. Stamm *et al.*, *J. Exp. Med.* **198**, 1361 (2003).
11. W. Kespichayawattana, S. Rattanachetkul, T. Wanun, U. Utaisincharoen, S. Sirisnha, *Infect. Immun.* **68**, 5377 (2000).
12. K. Breitbach *et al.*, *Cell. Microbiol.* **5**, 385 (2003).
13. D. Pantaloni, C. L. Clainche, M.-F. Carlier, *Science* **292**, 1502 (2001).
14. F. Frischknecht, M. Way, *Trends Cell Biol.* **11**, 30 (2001).
15. E. Gouin, M. D. Welch, P. Cossart, *Curr. Opin. Microbiol.* **8**, 35 (2005).
16. T. Suzuki, H. Miki, T. Takenawa, C. Sasakawa, *EMBO J.* **17**, 2767 (1998).
17. C. Egile *et al.*, *J. Cell Biol.* **146**, 1319 (1999).
18. T. Suzuki *et al.*, *J. Exp. Med.* **191**, 1905 (2000).
19. H. Ogawa, A. Nakamura, R. Nakaya, *Jpn. J. Med. Sci. Biol.* **21**, 259 (1968).
20. Materials and methods are available as supporting material on *Science* Online.
21. P. A. Giardini, J. A. Theriot, *Biophys. J.* **81**, 3193 (2001).
22. K. Uchiya *et al.*, *Mol. Microbiol.* **17**, 241 (1995).
23. S. Yoshida *et al.*, *EMBO J.* **21**, 2923 (2002).
24. S. Yoshida, C. Sasakawa, *Trends Microbiol.* **11**, 139 (2003).
25. B. Demers, P. J. Sansonetti, C. Parsot, *EMBO J.* **17**, 2894 (1998).
26. A. J. Barrett, N. D. Rawlings, *Biol. Chem.* **382**, 727 (2001).
27. V. Turk, B. Turk, D. Turk, *EMBO J.* **20**, 4629 (2001).
28. L. Cassimeris, *Curr. Opin. Cell Biol.* **14**, 18 (2002).
29. T. Pfeuffer, W. Goebel, J. Laubinger, M. Bachmann, M. Kuhn, *Cell. Microbiol.* **2**, 101 (2000).
30. The 3D-PSSM protein folding recognition server (www.sbg.bio.ic.ac.uk/~3dpssm).

Supporting Online Material

www.sciencemag.org/cgi/content/full/314/5801/985/DC1
Materials and Methods
Figs. S1 to S6
References

28 July 2006; accepted 29 September 2006
10.1126/science.1133174

HTRA1 Promoter Polymorphism in Wet Age-Related Macular Degeneration

Andrew DeWan,[1] Mugen Liu,[2]* Stephen Hartman,[3]* Samuel Shao-Min Zhang,[2]* David T. L. Liu,[4] Connie Zhao,[5] Pancy O. S. Tam,[4] Wai Man Chan,[4] Dennis S. C. Lam,[4] Michael Snyder,[3] Colin Barnstable,[2] Chi Pui Pang,[4] Josephine Hoh[1,2]†

Age-related macular degeneration (AMD), the most common cause of irreversible vision loss in individuals aged older than 50 years, is classified as either wet (neovascular) or dry (nonneovascular). Inherited variation in the complement factor H gene is a major risk factor for drusen in dry AMD. Here we report that a single-nucleotide polymorphism in the promoter region of *HTRA1*, a serine protease gene on chromosome 10q26, is a major genetic risk factor for wet AMD. A whole-genome association mapping strategy was applied to a Chinese population, yielding a *P* value of $<10^{-11}$. Individuals with the risk-associated genotype were estimated to have a likelihood of developing wet AMD 10 times that of individuals with the wild-type genotype.

Age-related macular degeneration (AMD) is the leading cause of vision loss and blindness among older individuals in the United States and throughout the developed world. It has a complex etiology involving genetic and environmental factors. AMD is broadly classified as either dry (nonneovascular) or wet (neovascular). The dry form is more common and accounts for about 85 to 90% of patients with AMD; it does not typically result in blindness. The primary clinical sign of dry AMD is the presence of soft drusen with indistinct margins (extracellular protein deposits) between the retinal pigment epithelium (RPE) and Bruch's membrane. The large accumulation of these drusen is associated with central geographic atrophy (CGA) and results in blurred central vision. About 10% of AMD patients have the wet form, in which new blood vessels form and break beneath the retina [choroidal neovascularization (CNV)]. This leakage causes permanent damage to surrounding retinal tissue, distorting and destroying central vision. The factors that underlie why some individuals develop the more aggressive wet form of AMD, while others have the slowly progressing dry type, are not yet understood.

Complement factor H (CFH) has been suggested to mediate drusen formation (*1*). In our previous whole-genome association study, in which the presence of large drusen was the primary phenotype under investigation, the CFH Y402H variant, in which Tyr^{402} is replaced by His, was shown to be a major genetic risk factor (*2*). More recently, it has been reported that the highest odds ratio for CFH Y402H was seen for cases with AMD grade 4 (i.e., the presence of CGA) in comparison with AMD grade 1 controls (*3*). An association between AMD and CFH Y402H, as well as other intronic CFH variants, has been demonstrated for more than ten different Caucasian populations (*4*–*7*).

Microtubule-Severing Activity of *Shigella* Is Pivotal for Intercellular Spreading

Sei Yoshida, Yutaka Handa, Toshihiko Suzuki, Michinaga Ogawa, Masato Suzuki, Asuka Tamai, Akio Abe, Eisaku Katayama and Chihiro Sasakawa

Science **314** (5801), 985-989.
DOI: 10.1126/science.1133174